Fabrication of a DRA Array Using Ceramic Stereolithography

Amelia Buerkle, *Student Member, IEEE*, Karl F. Brakora, *Student Member, IEEE*, and Kamal Sarabandi, *Fellow Member, IEEE*

***Abstract*—The purpose of this letter is to demonstrate monolithic fabrication of an array of dielectric resonator antennas (DRAs) using ceramic stereolithography. Design and measurements of a eight-by-eight array of rectangular DRAs composed of four monolithic four-by-four array blocks are presented. The array elements are designed over a ground plane and fed by a standard aperture-coupled microstrip corporate feed network. It is shown that the corporate feed, and not the DRAs, is mainly responsible for losses in the radiating structure.**

***Index Terms*—Antenna arrays, ceramic stereolithography, dielectric antennas.**

I. Introduction

The purpose of this research is to demonstrate the application of ceramic stereolithographic (CSLA) processing to the fabrication of dielectric antenna arrays. Recent research efforts have developed stereolithographic prototyping methods that achieve a dense, entirely ceramic end product. CSLA is a fully three-dimensional (3-D) additive layer-by-layer fabrication process that constructs parts from a photoreactive ceramic/monomer suspension. Since many ceramics exhibit low loss characteristics through millimeter-wave (MMW) frequencies and above, CSLA has enabled a range of solutions for MMW applications. It is an ideal process for monolithic construction of MMW subsystems composed of all-dielectric resonators, filters, waveguides, and antennas. Recently, CSLA has successfully been employed to fabricate the first ceramic Luneberg lens [1]. The variable dielectric profile of the Luneberg lens is realized by controlling the ceramic volume fraction through minor alterations to an isotropic periodic lattice.

Antenna arrays are good candidates for stereolithographic fabrication because of the increase in both difficulty and cost of individual element placement and bonding with increasing frequency. For example, automotive radar systems operating around 75 GHz are often implemented using printed circuit technology with patch antennas as radiating elements. Although patch arrays are both low cost and low profile, they are undesirable at high frequencies due to their low-radiation efficiency. The present approach combines the advantages of the monolithic structure resulting from stereolithographic processing and the high radiation efficiency of ceramic DRAs. Such arrays can be fed by an elaborate dielectric waveguide corporate feed or by a traditional microstrip feed network.

The array elements shown in this work are rectangular dielectric resonator antennas (RDRA). The basic array is a four-by-four element configuration. A larger, eight-by-eight design is made using the four-by-four arrays as building blocks. For the sake of simplicity, a microstrip corporate feed network is used to uniformly excite the array. A review of the design process for the antenna elements and the feed network is provided in Section II. Return loss and pattern measurement results are given in Section III. Conclusions and suggestions for future work are stated in Section IV.

II. Ceramic Stereolithography

In CSLA processing, a photoreactive ceramic suspension in monomer is cured using a UV laser over a prescribed area. This step is repeated layer-by-layer while the part is gradually submerged, creating a three-dimensional “green” part, which has a high volume fraction of ceramic. The remaining polymer is then removed through a binder-burnout at $350^\circ - 450\ ^\circ\mathrm{C}$ and sintering at $1600\ ^\circ\mathrm{C}$ [2]. The result is a pure ceramic structure.

The ceramic material used in the fabrication process for the array is 99.8% alumina $(\mathrm{Al_2O_3})$. Alumina has a loss tangent on the order of 10^{-4} and a permittivity of 9.7 through Ka-band. While the effective dielectric constant of the resonators may be altered by latent porosity or delamination errors, the biggest constraint on the DRAs is the warpage introduced by the binder-burnout process.

III. Design Process

A. DRA Array Elements

DRAs’ high efficiency and low profile make them attractive candidates for applications at microwave and MMW frequencies. In this case, RDRAs are also chosen as the antenna elements because they are able to provide fractional bandwidths on the order of 10% for materials with moderate relative permittivity values ($\varepsilon_\mathrm{r} <\sim 10$) [3]. This allows greater design flexibility and improved operational bandwidth for the array. Using the dielectric waveguide model [4] and the ceramic permittivity, the elements’ resonant frequency is predicted to be between 19 and 20 GHz for resonators that are 3.6 mm square by 1.8 mm tall.

The element spacing is 0.8λ at an operating frequency of 20 GHz. A monolithic four by four array structure is obtained by using thin ceramic support beams between adjacent RDRA

Manuscript received June 15, 2006; revised September 8, 2006.

The authors are with the University of Michigan Radiation Laboratory, Ann Arbor, MI 48109 USA (e-mail: abuerkle@eecs.umich.edu; kbrakora@eecs.umich.edu; saraband@eecs.umich.edu).

Color versions of Figs. 1–4 available online at http://ieeexplore.ieee.org.
Digital Object Identifier 10.1109/LAWP.2006.885167

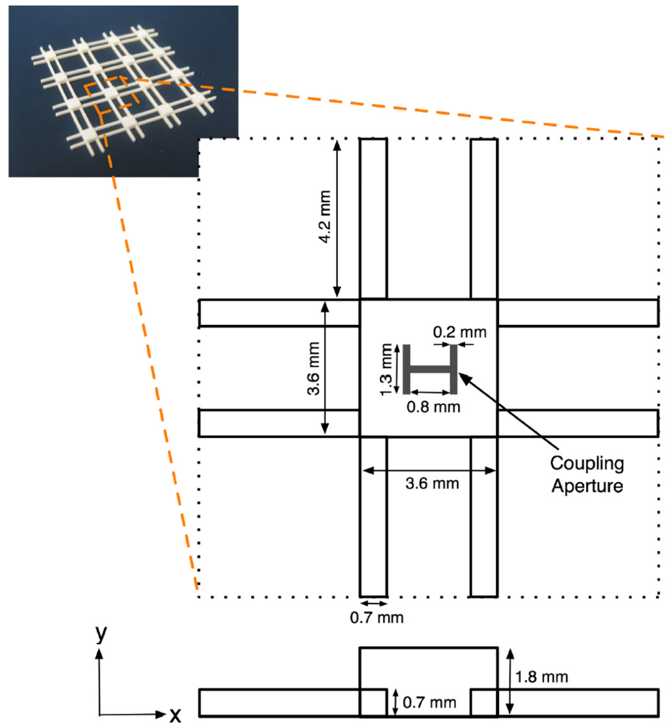

Fig. 1. Monolithic four-by-four array of RDRAs fabricated using CSLA. One cell of the array is shown in detail with the dimensions of the RDRA, supports, and coupling aperture.

elements. Two support beams with cross-sectional dimensions of 0.7 mm square are located on each side of the RDRA, connecting it to its nearest neighbors. It is assumed that the supports have minimal effect on the radiation pattern and input impedance of the elements; simulation results confirm this assumption. Fig. 1 is a photograph of the CSLA fabricated four-by-four array; one cell is also shown in detail with the dimensions of the RDRA, coupling aperture, and supports.

B. Microstrip Corporate Feed Network

Uniform element excitation is achieved using a corporate feed network and aperture coupling between the printed circuit and ceramic dielectric structure. Although the corporate feed suffers from low efficiency caused by long path lengths and reflections at the T-junctions, it is chosen in this study for its simplicity.

One quarter of the eight-by-eight feed network is shown in Fig. 2; the design is replicated to feed the sixty-four RDRA elements. A 50 Ω line is used at the input while 100 Ω line feeds each element. To achieve uniform phase distribution, the lower element of each pair of RDRAs is fed using an extra microstrip line length of 180°. The microstrip design is fabricated on 20 mil Roger's RT5880/Duroid ($\varepsilon_r = 2.2$, $\tan \delta_e = 0.0009$).

The coupling apertures, which are dogbone-shaped, are centered under the RDRAs. As reported in [5] the dogbone shape increases coupling by allowing a more uniform field distribution than a rectangular aperture. In addition, this geometry reduces back-radiation. The dimensions of the coupling apertures are shown in Fig. 1.

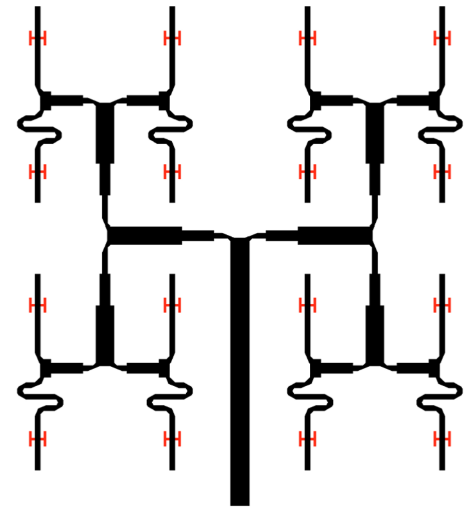

Fig. 2. Four-by-four microstrip feed network with dogbone-shaped coupling apertures. The design is replicated to feed the eight-by-eight array.

C. Simulation Notes

The four-by-four microstrip feed network is simulated using Agilent Advanced Design System (ADS). The simulation provides a means of checking uniformity in feeding amplitude and phase across the array. A single antenna element with a microstrip feed and ground plane is then modeled in Ansoft High Frequency Structure Simulator (HFSS). The aperture geometry and open-circuit microstrip stub length necessary to obtain a sufficient input match are determined. The four by four array is then simulated in HFSS by importing the feed network from ADS and including the remaining antenna components. The entire eight-by-eight configuration is not simulated because of the required computational effort.

D. Assembly

An aluminum fixture has been built in order to facilitate pattern measurement, keep the substrate flat, and simplify the coaxial to microstrip transition at the input. The arrays are attached by the supports to the ground plane of the substrate. The substrate is held in the measurement fixture with screws. Silver epoxy is also used around the frame to ensure electrical contact with the ground plane. Simulation and measurements indicate that the frame has a tendency to increase the sidelobe level. Fig. 3 is a photograph of the eight by eight array in the measurement fixture.

A small air gap between the ceramic array and the ground plane is a potential problem that is not included in simulation. The gap is caused by the combination of substrate warping and lack of flatness on the bottom of the arrays. During assembly, pressure is applied to establish contact at each element and minimize the air gap, effectively molding the flexible substrate material to whatever curvature exists on the bottom of the array. The air gap is estimated to be smaller than 25 μm.

To protect the feed and eliminate the possibility of any back-radiation, an aluminum plate is screwed onto the back of the aluminum fixture. The plate is approximately 3 mm away from the microstrip. The return loss does not significantly change when

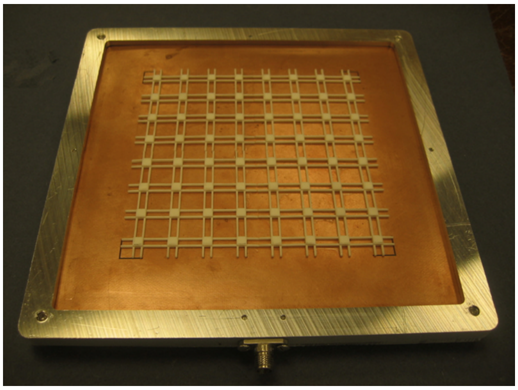

Fig. 3. The eight by eight array in the measurement fixture. Copper tape (not shown) is used around the border of the frame to ensure electrical contact with the ground plane.

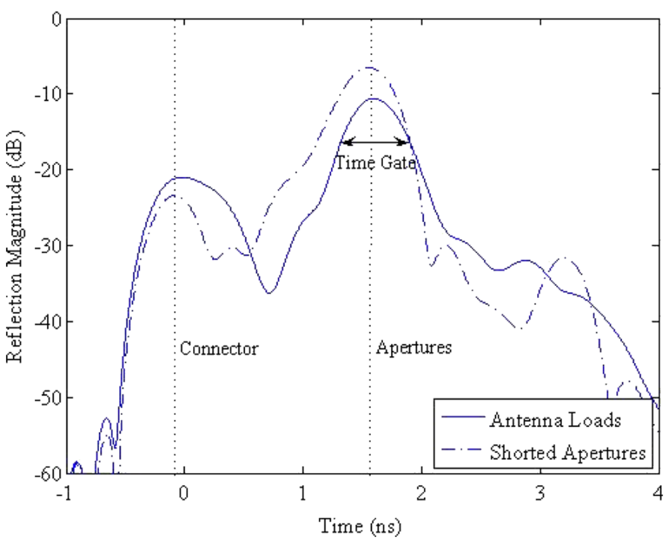

Fig. 4. Time domain reflections of feed network with shorted coupling apertures and with antenna loads.

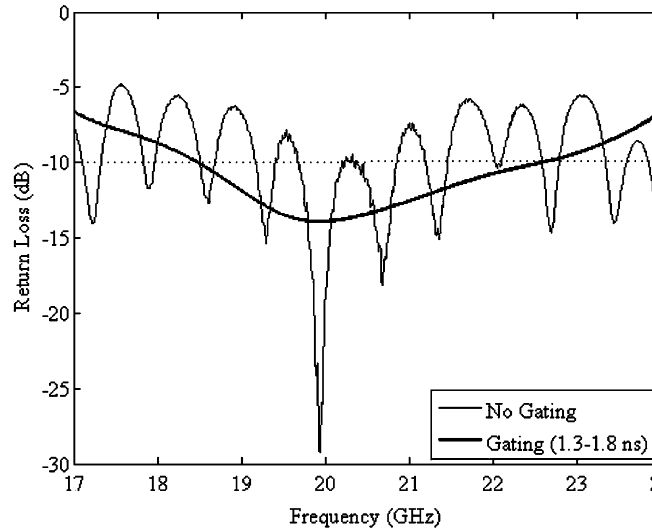

Fig. 5. Return loss of the eight-by-eight array in the measurement fixture with the back plate.

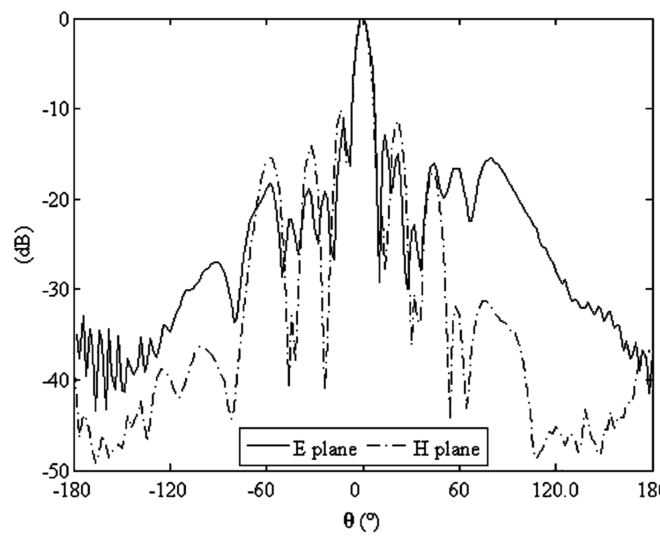

Fig. 6. E- and H-plane radiation patterns at 20 GHz for the eight-by-eight array in the measurement fixture. Absorber is placed around the frame periphery in reduce its effects on the pattern.

the plate is in place, indicating that the currents on the microstrip are not significantly altered by its presence.

IV. Measurement Results

A. Estimation of Loss in the Feed Network

The array return loss was measured using an Agilent 8722ES vector network analyzer. The loss in the feed network is estimated using time domain measurements. A return loss measurement is done with the coupling apertures short-circuited, before the RDRA arrays are glued in place. The results are shown as the dashed curve in Fig. 4; the corresponding frequency range is 17.5–21 GHz. Using the magnitude of the reflection from the shorted apertures, along with the magnitude of the reflection at the input connector, the loss in the feed network is estimated to be 3.2 dB.

B. Return Loss

The measured return loss with and without time gating for the array is shown in Fig. 5. In the first curve, corresponding to no time gating, achieving a wideband match that is better than 10 dB is difficult because of reflections within the feed network. The nulls occur approximately every 600 MHz, corresponding to a microstrip length of about 20 cm, or about the total distance between the coaxial connector and the RDRAs aperture. The second, bold curve in Fig. 5 is the return loss after time gating the reflected signal. As indicated by the time domain measurement with the antenna loads in place (the solid curve in Fig. 4), the time gate surrounds the peak corresponding to reflections from the RDRAs (1.3–1.8 ns). The match to the RDRA elements is found to be approximately 8 dB after measuring 6.4 dB of total loss in the round trip from the coaxial connector to the RDRA feed points. As mentioned, the lack of a perfect match can be attributed to the existence of very small air gaps, which seem nearly unavoidable over such a large area.

C. Radiation Patterns

The radiation patterns of the array in the principal planes are measured in the anechoic chamber at the University of Michigan. The measured E $(y-z)$ and H $(x-y)$ plane patterns at 20 GHz are shown in Fig. 6. The beamwidth is approximately 9°. The sidelobe level is -12 dB in the E plane and -10 dB in the H plane. A cause of higher than expected sidelobes can be attributed to the metallic frame and residual phase and amplitude errors introduced by the airgaps. It was verified that once the frame was covered by absorbers the side-lobe levels could be reduced slightly (1–2 dB).

The observed pattern asymmetry is also a result of the residual errors in feeding phase and amplitude. The measured gain is 21.3 dBi. For reference, an aperture antenna of the same size and an aperture efficiency of 81% would have about 26 dB of gain [6]. The 4.7 dB difference is due to losses in the feed network (3.2 dB) and inadequate matching at the antenna elements caused by array misalignment and the air gap. The ceramic RDRA elements contribute negligible loss. To make the array less susceptible to residual feeding errors and to the effects of air gaps, smaller element spacing is recommended.

V. Conclusion

A new application for CSLA processing has been demonstrated. The advantage of the monolithic array structure is evident in the straightforward extension of a four-by-four configuration into an eight-by-eight array. The measured results indicate the array behaves in essentially the same way as an array with individual elements.

There are simple improvements that could be made to obtain superior performance. An inflexible substrate material, such as Rogers TMM3, could be used instead of Duroid. Initially, achieving adequate flatness on the bottom of the array was a potential difficulty in fabrication; the flexible Duroid substrate was chosen to make up for any lack of flatness. However, the fabricated ceramic arrays are sufficiently flat for the frequency of operation. An inflexible substrate would reduce the need for a measurement fixture and simplify analysis of the radiation patterns. The array performance could also be improved by using smaller element spacing and an alternative feed network topology.

The design is a first step in using CSLA in antenna array applications. Future work will include developing a ceramic feed network to achieve much higher efficiency and eliminating the air gap problem.

Acknowledgment

The authors would like to thank W. Zimbeck at Technology Assessment and Transfer, Inc. (www.techassess.com).

References

[1] K. Brakora and K. Sarabandi, “Design of 3-D monolithic MMW antennas using ceramic stereolithography,” IEEE Trans. Antennas and Propagat., submitted for publication.

[2] P. F. Jacobs, *Stereolithography and Other RP&M Technologies*. New York: ASME Press, 1996.

[3] A. Petosa, A. Ittipiboon, Y. M. M. Antar, D. Roscoe, and M. Cuhaci, “Recent advances in dielectric-resonator antenna technology,” *IEEE Antennas Propagat. Mag.*, vol. 40, pp. 35–48, Jun. 1998.

[4] R. K. Mongia and A. Ittipiboon, “Theoretical and experimental investigations on rectangular dielectric resonator antennas,” *IEEE Trans. Antennas Propagat.*, vol. 45, pp. 1348–1356, Sep. 1997.

[5] D. M. Pozar and S. D. Targonski, “Improved coupling for aperture coupled microstrip antennas,” *Electron. Lett.*, vol. 27, pp. 1129–1131, Jun. 1991.

[6] C. Balanis, *Antenna Theory*. New York: Wiley, 1997, ch. 2.